International Journal of Nanomedicine

Dovepress
Taylor & Francis Group

Open Access Full Text Article

ORIGINAL RESEARCH

Dual-Stage Targeted Oral Drug Loaded Nanostructured Lipid Carriers Enhance the Efficacy of Ulcerative Colitis

Meijia Liu, Junyi Cui, Hanqing Li, Jie Yang, Guoyun Liu

State Key Laboratory of Macromolecular Drugs and Large-Scale Preparation, School of Pharmaceutical Sciences and Food Engineering, Liaocheng University, Liaocheng, Shandong, 252059, People's Republic of China

Correspondence: Guoyun Liu; Jie Yang, Email liuguoyun@lcu.edu.cn; yangjie3@lcu.edu.cn

Purpose: Ulcerative colitis (UC) is a non-specific inflammatory intestinal disease with long course and easy recurrence, which is one of the refractory diseases. In the previous work, *para*-quinone methide compound *p*-QM-**1i** was found to be a potential anti-UC drug in UC mice; however, its water solubility was poor, and the oral dosage was high. In this study, in response to these shortcomings, an oral, actively targeted, and drug-loaded nanostructured lipid carrier (NLC) was constructed, and the dual-stage targeted design was performed on it.

Methods: Firstly, the *p*-QM-**1i**-loaded NLC surface was modified with infliximab (IFX) (*p*-QM-**1i**-IFX-NLC), which can target highly expressed TNF-α in inflammatory cells or tissues; secondly, *p*-QM-**1i**-IFX-NLC was coated with Eudragit S100 (S100-**1i**-IFX-NLC), which can achieve specific release in the colon and protect NLC from interference from the gastrointestinal environment.

Results: The experimental results suggested that the dual-stage targeted design of S100-**1i**-IFX-NLC can effectively increase the solubility of *p*-QM-**1i**, allowing S100-**1i**-IFX-NLC to target the colon and *p*-QM-**1i**-IFX-NLC to target the inflammatory tissue, increasing the aggregation of *p*-QM-**1i** in the colon, enhancing the efficacy of *p*-QM-**1i**, reducing the usage of *p*-QM-**1i**, and increasing safety.

Conclusion: The construction of Eudragit S100-coated *p*-QM-**1i**-loaded IFX-modified NLC (S100-**1i**-IFX-NLC) was effective and can improve the therapeutic effect of free drugs on UC.

Keywords: ulcerative colitis, nanostructured lipid carriers, target delivery, TNF-α, colon specific release

Introduction

Ulcerative colitis (UC) is a pathological condition of unknown etiology, characterized by non-specific inflammation and ulceration of the rectal and colonic mucosa. The main clinical symptoms include abdominal pain, diarrhea, severe diarrhea, and mucous purulent bloody stools;[1–3] and this disease has a long course of illness, often prone to recurrence, and is generally a lifelong recurrent disease.[4] At present, the etiology and pathogenesis of this disease are not yet clear, and the treatment is difficult. It has been listed as one of the modern difficulties to treat diseases by the World Health Organization; also known as "green cancer".

Quinone methylates are a class of bioactive compounds that can be used in medicine as antiviral, antifungal, antibacterial, anti-inflammatory, and antioxidant agents.[5] In our previous work,[6,7] we synthesized a series of quinone methylation derivatives. In the lipopolysaccharide (LPS)-induced inflammatory Raw264.7 cell model, the *para*-trifluoromethyl substituted quinone methide derivative **1i (***p*-QM-**1i)** showed the best activity in inhibiting LPS-induced excessive NO production. Moreover, *p*-QM-**1i** can effectively inhibit the expression of inflammation-related promoter protein toll-like receptor 4 (TLR4), pro-inflammatory cytokines interleukins (IL)-6 and tumour necrosis factor (TNF)-α, inflammasome NOD-like receptor family pyrin domain-containing 3 (NLRP3), and cysteine aspartic acid-specific protease (Caspase1). Furthermore, in the mouse model of UC induced by sodium dextran sulfate (DSS), the active derivative *p*-QM-**1i** can inhibit DSS-induced colon shortening and reverse DSS-induced pathological changes in

Received: 21 June 2025
Accepted: 10 October 2025
Published: 18 October 2025

Graphical Abstract

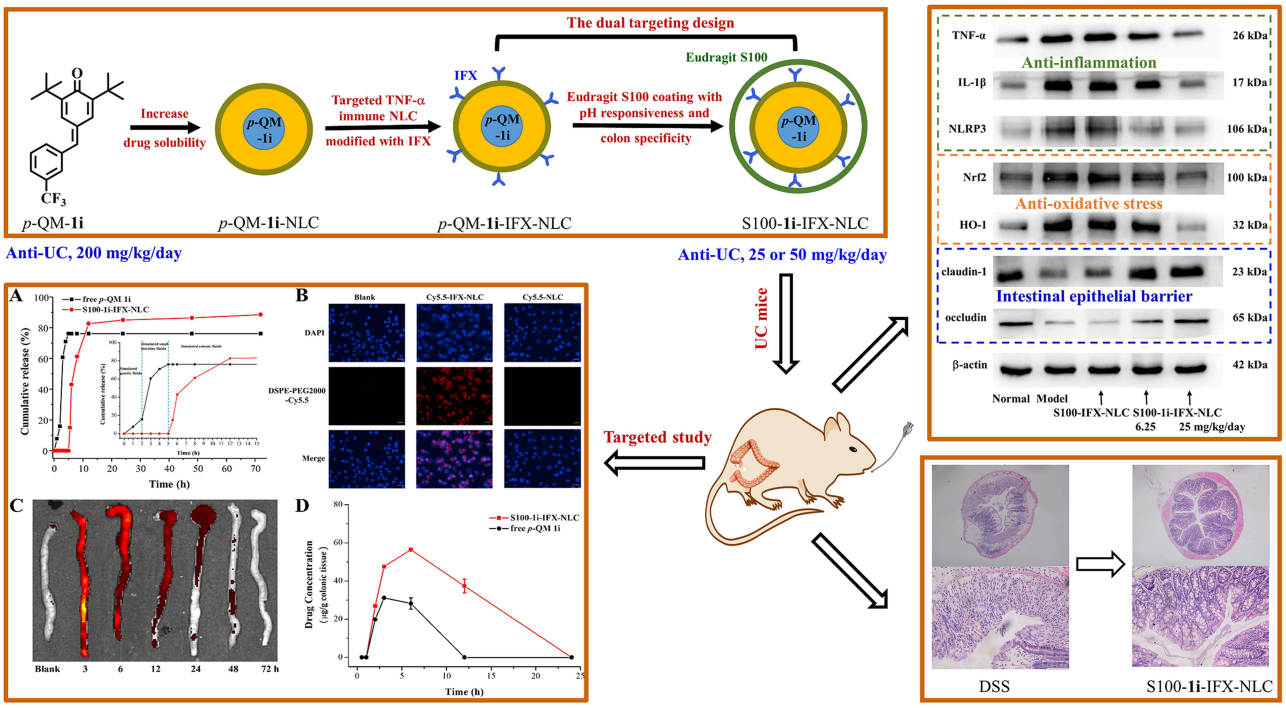

colon cancer tissue. In addition, *p*-QM-**1i** can effectively inhibit oxidative stress, inflammation, and cell apoptosis in UC mice, and effectively reverse the damage of DSS to the liver and kidneys of mice, providing a protective effect on the liver and kidneys of mice. These results indicated that *p*-QM-**1i** was an effective anti-inflammatory agent with great potential as an anti UC drug. However, as an organic small molecule compound, *p*-QM-**1i** had very poor water solubility; the dosage of the drug administered orally to mice was relatively high, at 200 mg/kg; and it did not have targeting ability.

Nanoparticles can increase the solubility of non-water soluble drugs, reduce drug usage, and thus reduce side effects. Nanostructured lipid carriers (NLCs) are a type of lipid nanoparticle after solid lipid nanoparticles (SLNs), in which a portion of solid lipids are replaced by liquid lipids, allowing for the encapsulation of more drugs.[8–11] Immune NLC is produced by the binding of antibodies to NLC, which can achieve targeted drug delivery through antibodies. TNF-α is an important target of autoimmune diseases, and its molecules exist in two forms: transmembrane TNF-α (tmTNF-α) and secreted TNF-α (sTNF-α). tmTNF-α is distributed in the form of membrane proteins on cells that secrete TNF-α. Infliximab (IFX) is a human mouse chimeric monoclonal antibody that inhibits TNF-α. It can quickly form a stable complex with TNF-α and terminate the biological activity and signaling of TNF-α. We designed IFX modified immune NLC, hoping that it can bind to TNF-α in the inflamed colon tissue of the lesion, allowing the drug loaded NLC to reach the vicinity of the lesion and targeted release the drug in the inflamed colon of the lesion. In order to improve the active targeting of NLC on UC tissue, the TNF-α inhibitor IFX was combined with the surface of NLC, which is rarely reported and has certain innovation.

The oral route is a simple, safe, and easily accepted way of taking medication.[8–11] However, the antibodies attached to the immune NLC face many difficulties in oral administration due to the strong acidic gastric environment and susceptibility to enzymatic degradation in the intestine.[12–14] Eudragit S100 is a pH responsive pharmaceutical excipient that has been approved by the FDA for use in oral formulations. Eudragit S100 is mainly composed of poly (methacrylic acid) and poly (methyl methacrylate), with a carboxylic acid-to-ester ratio of approximately 1:2,[15,16] which is the principle behind Eudragit S100's pH-dependent colon targeted drug release. In the stomach (pH 2–3) and small intestine (pH 6.5–7),[16–18] due to its free

carboxylic acid form, the polymer exhibits a stable structure and is insoluble; in the colon (pH 7.0–8.0),[16–18] carboxyl groups (COOH) ionize into carboxylic acid anions (COO^-), increasing the water solubility of the polymer.[19,20] Using Eudragit S100 to coat immune NLC can maintain its stability when passing through the stomach and small intestine and specifically release immune NLC into inflamed colon,[12] enabling targeted release of loaded drugs by immune NLC.[12,20–22]

In this study, we encapsulated the active drug *p*-QM-**1i** with NLC (*p*-QM-**1i**-NLC) to enhance its solubility. In order to achieve targeted release of active drug *p*-QM-**1i** in inflammatory colon lesions, IFX modification was performed on *p*-QM-**1i**-NLC to prepare immune NLC (*p*-QM-**1i**-IFX-NLC). Furthermore, in order to address the adverse gastrointestinal conditions faced by oral medication, such as strong acidic gastric juice and a large amount of digestive enzymes, Eudragit S100 coating was applied to the immune NLC, allowing it to smoothly pass through the gastrointestinal tract and be targeted for release in the colon (Figure 1). We evaluated the nanostructure character, anti-UC activity, active targeting, and toxic activity of Eudragit S100-coated *p*-QM-**1i**-loaded infliximab-modified NLC (S100-**1i**-IFX-NLC), hoping to improve the targeting of active small molecule *p*-QM-**1i**, reduce drug usage, and minimize toxic side effects.

Materials and Methods

Preparation and Characterization of S100-1i-IFX-NLC

p-QM-1i-NLC

According to Table S1, the solid liposomes were weighed into a centrifuge tube, and dissolved with 5 mL of methanol. A certain amount of *p*-QM-**1i** was dissolved in liquid lipids under heating conditions. Mix solid lipid solution and liquid lipid solution. The mixture was subjected to vacuum distillation until the lipids adhere to the inner wall of the round bottom flask in the form of a lipid film at 75°C, −0.1 MPa and 80 rpm in a 100 mL round bottom flask. Then, continue vacuum distillation for 30 minutes to completely remove methanol. Two-milliliter PBS (10 mM, pH 7.4) was added to the round bottom flask, and the mixture was hydrated at −0.01 MPa for 20 minutes. The lipid membrane was shaken down by ultrasound. Liposomes were collected, and PBS was added to a total volume of 2 mL. Subsequently, the liposomes were crushed using the ultrasonic cell disruptor at 25 kHz and 4°C for 6 minutes. Afterwards, a manually pushed liposome extruder was used to manually extrude liposomes 21 times through a 200 nm pore size polycarbonate membrane. Then, liposomes were added to a 1000 MWCO dialysis bag and dialyzed in PBS buffer (three times water) for 12 hours, with fresh buffer replaced every 4 hours. The particle size, potential, and PDI of the dialyzed liposomes were measured for subsequent experiments.

p-QM-1i-IFX-NLC

The IFX in PBS (10 mM, pH 8.0) was mixture with Traut reagent (2-iminothiolane) at a molar ratio of 1:20 at 4°C for 4 hours, to facilitate the free amino sulfurization of IFX. Sulfurized IFX were dialyzed (1000 MWCO) in PBS (10 mM, pH 7.4) at 4°C overnight, to remove excess Traut reagent. Sulfurized IFX was incubated with *p*-QM-**1i**-NLC at a molar ratio of 1.5:1 at 4°C for 24 hours. Unbound Sulfurized IFX was removed by dialysis using a 3000 MWCO dialysis bag at 4°C overnight.

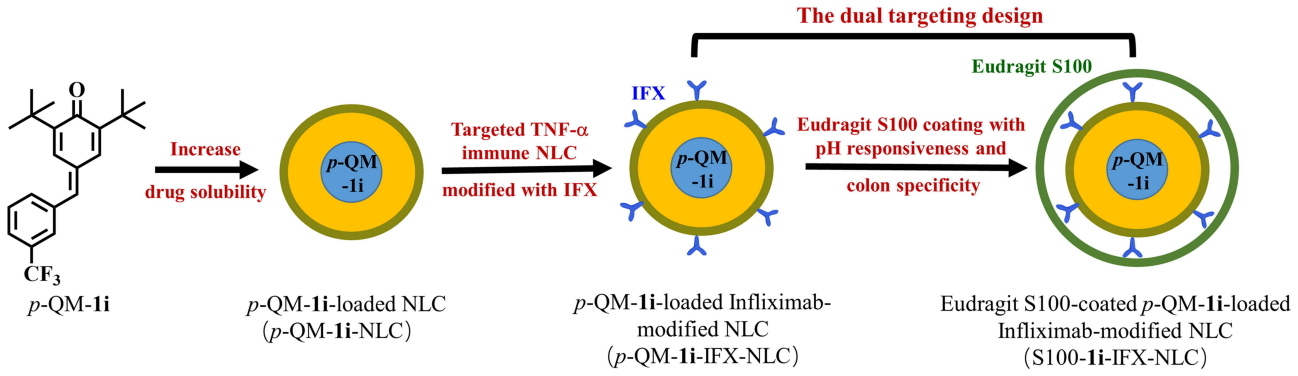

Figure 1 Design concept of S100-**1i**-IFX-NLC.

https://doi.org/10.2147/IJN.S548696

S100-1i-IFX-NLC

Freshly prepared blank or *p*-QM-**1i**-loaded IFX-NLC (2.5 mg/mL) was added dropwise to an equal volume of 0.2% w/v Eudragit S100 in PBS (10 mM, pH 7.0). The mixture was stirred at 4°C for 0.5 hour, and then ultrafiltered at 4000 g and 4°C for 45 minutes. The obtained coated immune NLC was redispersed in the original volume of PBS (10 mM, PH 7.0).

Identification of Nanoparticle Characteristics

The particle size, PDI and Zeta potential were analyzed using dynamic light scattering (Zetasizer Nano ZSE, Malvern, UK). DLS detection was equipped with an integrated 4 mV He-Ne laser (633 nm) and backscattering detection with a scattering angle of 173°.

Ten microliter DMSO and 20 μL Tritron-X 100 were added to 50 μL dialyzed *p*-QM-**1i**-NLC solution. The mixture was vortexed for 30 seconds, and allowed to stand for 30 minutes to break the emulsion. Then, 320 μL acetonitrile was added to the mixture and vortexed. After centrifugation at 12000 g for 10 minutes, the supernatant was taken to determine the concentration of *p*-QM-**1i** using HPLC, and the encapsulation efficiency (EE) and drug loading content (DLC) of *p*-QM-**1i-NLC** were further calculated.

The EE and DLC of *p*-QM-**1i**-NLC reflected the capacity of NLC to load *p*-QM-**1i**. The modification of IFX and the coating of S100 had no effect on the capacity of NLC to load *p*-QM-**1i**. Therefore, there was no repeated measurement and evaluation of the loading capacity of nanomaterials on *p*-QM-**1i**.

EE% = (the amount of Drug encapsulated in nanoparticles/total drug dosage) x 100%

DLC% = (the amount of Drug encapsulated in nanoparticles/total mass of liposomes) x 100%

Immune Characteristic Identification of p-QM-1i-IFX-NLC

(1) Connection efficiency of IFX

The protein concentration of IFX in dialyzed *p*-QM-**1i**-IFX-NLC was detected using the BCA assay kit, and the result was used to calculate antibody ligation efficiency.[23–25]

Antibody conjugation efficiency% = (the amount of antibodies contained in liposomes/number of sites) x 100%

(2) Antibody integrity

Sodium dodecyl sulfate polyacrylamide gel electrophoresis (SDS-PAGE) (12%) was carried out as the general process, and the gel was stained with coomassie blue. The primary structure integrity of IFX was analyzed by comparing the bands of the free IFX and the IFX bound on the immune *p*-QM-**1i**-IFX-NLC.

Free IFX, thiolated IFX, and *p*-QM-**1i**-IFX-NLC at equivalent concentrations were performed fluorescence analysis using a fluorescence spectrophotometer. (Ex, 280 nm; Em, 300 to 420 nm) Guanidine hydrochloride (6 M), as the denaturing agent, was added to the above three solutions to evaluate the suppression of fluorescence and the displacement of the maximum wavelength to less energetic wavelengths.

Evaluation of Anti-UC Activity

Animal

Eight-week-old Balb/c mice (18–20 g, male) were purchased from Jinan Pengyue Experimental Animal Breeding Co., Ltd. Mice are allowed to drink and eat freely in a 12 hours light dark cycle and an environment of 23 ± 2°C. Animal experiments are strictly conducted in accordance with the National Laboratory Animal Care and Use Guidelines. The experimental plan has received support from the Ethics Committee of Liaocheng University (No 2023022718).

Anti-UC Mouse Experiment

After the adaptation for seven days, the mice were randomly divided into seven groups (8 mice/group): (1) normal group, (2) model group, (3) S100-IFX-NLC-treated group and (4–7) 6.25, 12.5, 25 or 50 mg/kg S100-**1i**-IFX-NLC-treated groups. Due to the possibility of mice dying from rectal bleeding, there were 12 mice in the model group. The number of mice in other groups was 8. Except the normal group, other mice were allowed to freely access 3% DSS aqueous solution for 10 days. From the fifth to tenth day, mice in S100-IFX-NLC-treated group were orally administered with 0.5 mL of S100-IFX-NLC every day; mice in S100-**1i**-IFX-NLC-treated groups were orally administered with 0.0625, 0.125, 0.25 or 0.5 mL of S100-**1i**-IFX-NLC containing 6.25, 12.5, 25 or 50 mg/kg *p*-QM-**1i** every day. Mice in the normal group

were orally administered with 0.5 mL of PBS every day. After intragastric administration on the tenth day, the mice were fasted for 12 hours. After blood was taken from the eyeball, the mice were decapitated and killed, and taken the organs.

Serum Index Detection

Serum indicators aspartate transaminase (AST), alanine aminotransferase (ALT), blood urea nitrogen (BUN) and creatinine (CRE) were measured using commercially available assay kits the aspartate transaminase (AST)/glutamic oxaloacetic transaminase (GOT) activity detection kit (E2023, Applygen), the alanine aminotransferase (ALT)/glutamate pyruvate transaminase (GPT) activity detection kit (E2021, Applygen), the urea (BUN) assay kit (C013-1-1, Nanjing Jiancheng) and the creatinine (CRE) assay kit (C011-2-1, Nanjing Jiancheng), respectively.

Detection of Oxidative Stress Indicators in the Colon

Oxidative stress indicators malondialdehyde (MDA) and catalase (CAT) in the colon were measured using commercially available assay kits lipid peroxidative MDA assay kit (S0121M, Beyotime) and the catalase assay kit (A007-2-1, Nanjing Jiancheng).

For the determination of myeloperoxidase (MPO),[26] 60 μL of working solution (0.0005% *o*-diaminodiphenylenediamine dihydrochloride and 0.1% hydrogen peroxide in PBS (50 mM, pH 6.0)) was added to 40 μL of colon tissue supernatant. After mixing, the mixed solution was immediately measured at 460 nm at 25°C using a microplate reader. The change of 5.65×10^{-3} in absorbance was equivalent to one unit of MPO activity. MPO activity was expressed in U/mg pro.

Histopathological Analysis

Following the general process, colon tissue was fixed with 4% paraformaldehyde (Beyotime), embedded in paraffin and sliced. After staining with hematoxylin and eosin (Beyotime), images were taken using an Olympus microscope (BX53+DP80).

Western Blot

Following the general process, colon tissue supernatant was performed Western blot experiment. The primary antibodies were as follows: TNF-α (WL01581, Wanleibio), IL-1β (WL00891, Wanleibio), NLRP3 (WL02635, Wanleibio), nuclear factor erythroid 2-related factor 2 (Nrf2) (WL02135, Wanleibio), heme oxygenase 1 (HO-1) (WL02400, Wanleibio), claudin-1 (WL 03073, Wanleibio), occludin (WL01996, Wanleibio), β-actin (GB15003, Servicebio). The secondary antibodies were as follows: HRP-labeled Goat Anti-Rabbit IgG (H+L) (A0208, Beyotime). The dilution concentration of all first antibodies used in the Western blot experiment was 1:1000.

Active Targeting Determination of NLC

Drug Release of S100-1i-IFX-NLC at Different pH Levels

(1) According to the Chinese Pharmacopoeia to prepare artificial gastrointestinal fluid.

Artificial gastric juice: 234 mL of concentrated hydrochloric acid was diluted with water to 1000 mL to obtain 9.5–10.5% dilute hydrochloric acid. Eight hundred milliliters of water and 10 g of gastric protease were added to 16.4 mL dilute hydrochloric acid, and then the mixture was shaken and diluted with water to 1000 mL.

Artificial small intestine fluid: 500 mL water was added to 6.8 g KH_2PO_4, and 0.1 M hydrochloric acid was added to the mixed solution to adjust pH to 6.8. Ten-gram trypsin was dissolved in water and then was added to the above solution. Water was added to the mixed solution to 1000 mL.

Artificial colon fluid: 5.59 g K_2HPO_4 and 0.41 g KH_2PO_4 were dissolved in water to obtain 1000 mL solution.

(2) Firstly, 0.5 mL of 2.232 mg/mL S100-**1i**-IFX-NLC was placed in the dialysis bag (10000 MWCO), and was released in 50 mL of simulated gastric juice for 2 hours. Secondly, the dialysis bag was transferred to 50 mL of simulated small intestine fluid and was released for 3 hours. Finally, the dialysis bag was transferred to 50 mL of simulated colon fluid and was released until the end of the 72 hours experiment. Throughout the experiment, the experimental setup was placed in a culture shaker at 100 rpm and 37°C for release testing. About 0.5 mL of release medium was collected at 0.5, 1, 2, 3, 4, 5, 6, 8, 24, 48 and 72 hours in the experiment, and the same volume of fresh release medium was added.

Active Targeting Determination in the LPS-Induced Inflammatory Raw264.7 Cells Model

The Raw264.7 cell line was obtained from the National Collection of Authenticated Cell Cultures of the Chinese Academy of Sciences, and cultured in DMEM (Hyclone) medium containing 10% fetal bovine serum (Gibco) and 1% penicillin–streptomycin solution (Beyotime) in a 37°C and 5% CO_2 incubator (Thermo Scientific Heraciu 150i).

According to the method reported in the literature[27–31] with modifications, NLC was fluorescently labeled and used for targeted studies. One-milligram DSPE-PEG2000 in the preparation method was replaced with 1mg Cy5.5-DSPE-PEG2000. Two milliliters of Raw264.7 cells at a density of 1.5×10^5 cells/mL was inoculated in a 6-well plate. After 24 hours, cells were inoculated in fresh medium containing 1 μg/mL LPS for another 24 hours. Then, 100 μL Cy5.5-IFX-NLC or Cy5.5-NLC was added and inoculated for 3 hours. After removing the culture medium, the cells were washed twice with PBS and fixed with 2 mL of 4% paraformaldehyde solution (Beyotime) for 10 minutes. After removing the fixative, the cells were washed twice with PBS and added a drop of anti-fade mounting medium with DAPI. Stained cell samples were photographed using a fluorescence microscope (Olympus).

Two milliliters of Raw264.7 cells at a density of 1.5×10^5 cells/mL was inoculated in a 6-well plate. After 24 hours, cells were inoculated in fresh medium containing 1 μg/mL LPS for another 24 hours. Then, 100 μL Cy5.5-IFX-NLC or Cy5.5-NLC was added and inoculated for 3 hours. After removing the culture medium, the cells were washed twice with PBS and collected. Then, the cells were analyzed using flow cytometry.

Active Targeting Determination in the DSS-Induced UC Mouse Model

(1) Fluorescence imaging

After the adaptation for seven days, mice freely accessed 3% DSS aqueous solution. Starting from the fifth day, mice were orally administered with 0.5 mL of Cy5.5-S100-IFX-NLC once. After 3, 6, 12, 24, 48 and 72 hours of gavage in different groups, mice were euthanized simultaneously, and their colons were removed. The feces in the colon were washed with cool PBS and then photographed using the in vivo imaging system. In addition, after 3, 6, 12, 24, 48 and 72 hours of gavage in different groups, another group of mice were euthanized simultaneously, their gastrointestinal tract were removed, and then photographed using the in vivo imaging system.

(2) Quantitative measurement

After the adaptation for seven days, mice freely accessed 3% DSS aqueous solution. Starting from the fifth day, mice were orally administered with 0.5 mL of 50 mg/kg free *p*-QM-**1i** in carboxymethylcellulose sodium (0.5%) solution (P1346637, Adamas-beta) or 0.5 mL of S100-**1i**-IFX-NLC containing 50 mg/kg *p*-QM-**1i** once. After 0.5, 1, 2, 3, 6, 12, 24 hours of gavage in different groups, mice were euthanized, and their colons were removed. Colonic tissue was homogenized in PBS and then mixed with an equal volume of ethyl acetate. The mixture was centrifuged at 12000 g and 4°C for 10 minutes, and collected the supernatant. An equal volume of ethyl acetate was added to the precipitate and then collected the supernatant. This process was repeated twice. All the ethyl acetate solutions were combined and evaporated under reduced pressure. Four hundred microliters of methanol was added to the obtained solid, and the concentration of *p*-QM-**1i** of samples was determined with high performance liquid chromatography (HPLC, Agilent Technologies 1260 Infinity, Germany) (Eluent, methonal: H_2O = 90:10; flow rate, 1 mL/min; λ, 348 nm; retention time, 16.223 min).

Statistical Analysis

All experiments were conducted independently at least three times. The number of mice in the experiment was 8. Data were expressed as mean ± SD. The statistical significance analysis of experimental data was conducted using the one-way analysis of variance test and dunnett test in GraphPad Prism software. $p < 0.05$ was considered statistically significant.

Results

Preparation and Characterization of p-QM-1i-NLC, p-QM-1i-IFX-NLC and S100-1i-IFX-NLC

p-QM-1i-NLC

The *p*-QM-**1i**-NLC was prepared using thin film dispersion method. The types and proportions of lipids used in the preparation of *p*-QM-**1i**-NLC were shown in Table S1. According to dynamic light scattering analysis, the particle size of

Table 1 Characterization of *p*-QM-**1i**-NLC and S100-**1i**-IFX-NLC

NPs	Size (d.nm)	PDI	Zeta (mV)	EE (%)	DLC (%)
p-QM-**1i**-NLC	136.38±0.74	0.116±0.012	−13.73±0.44	86.51±2.22	7.70±0.20
S100-**1i**-IFX-NLC	194.20±2.03	0.223±0.015	−12.8±0.51	/	/

p-QM-**1i**-NLC was 136.38 nm, with a PDI of 0.116 (Table 1), indicating that the particle size distribution of *p*-QM-**1i**-NLC was uniform. And *p*-QM-**1i**-NLC had good storage stability within 14 days, as their particle size, PDI, and zeta potential remain largely unchanged (Figure 2A–D). In addition, the EE of *p*-QM-**1i**-loaded NLC was 86.51%, and the DLC was 7.70% (Table 1). This indicated that *p*-QM-**1i**-NLC can provide sufficient space to accommodate drug molecules and prevent their leakage.

p-QM-1i-IFX-NLC

Furthermore, IFX was modified on the surface of *p*-QM-**1i**-NLC to construct the immune NLC (*p*-QM-**1i**-IFX-NLC) with active targeting ability, which can target inflammatory cells or tissues. In the preparation of immune NLC, the antibody conjugation efficiency could be maintained at 90%, as analyzed by BCA (See Table S2).

And, in order to determine the antibody integrity after conjugation, the primary and tertiary structures of IFX antibody on the surface of *p*-QM-**1i**-IFX-NLC were analyzed. Through the analysis of SDS-PAGE, the IFX monoclonal antibody modified on the *p*-QM-**1i**-IFX-NLC surface showed two bands (heavy chain and light chain) on the electrophoresis gel, which was the same as the electrophoresis pattern of the free IFX antibody (Figure 2E). So the IFX antibody modified on the surface of *p*-QM-**1i**-IFX-NLC was not damaged, maintaining the integrity of the IFX primary structure.

Analyze the integrity of the tertiary structure of antibodies through fluorescence visible light spectroscopy.[32,33] Under excitation at 280 nm, IFX monoclonal antibody exhibits the maximum fluorescence intensity at 340.40 ± 0.60 nm (Figure 2F and Table S3), attributed to the presence of aromatic amino acid residues in the structure of IFX. Under the action of the deformation agent guanidine hydrochloride, the fluorescence intensity of IFX monoclonal antibody is suppressed, and the maximum fluorescence emission wavelength increases and shifts to 358.80 ± 0.20 nm. The thio-IFX antibody and the functionalized IFX antibody connected to *p*-QM-**1i**-IFX-NLC also exhibited the maximum fluorescence

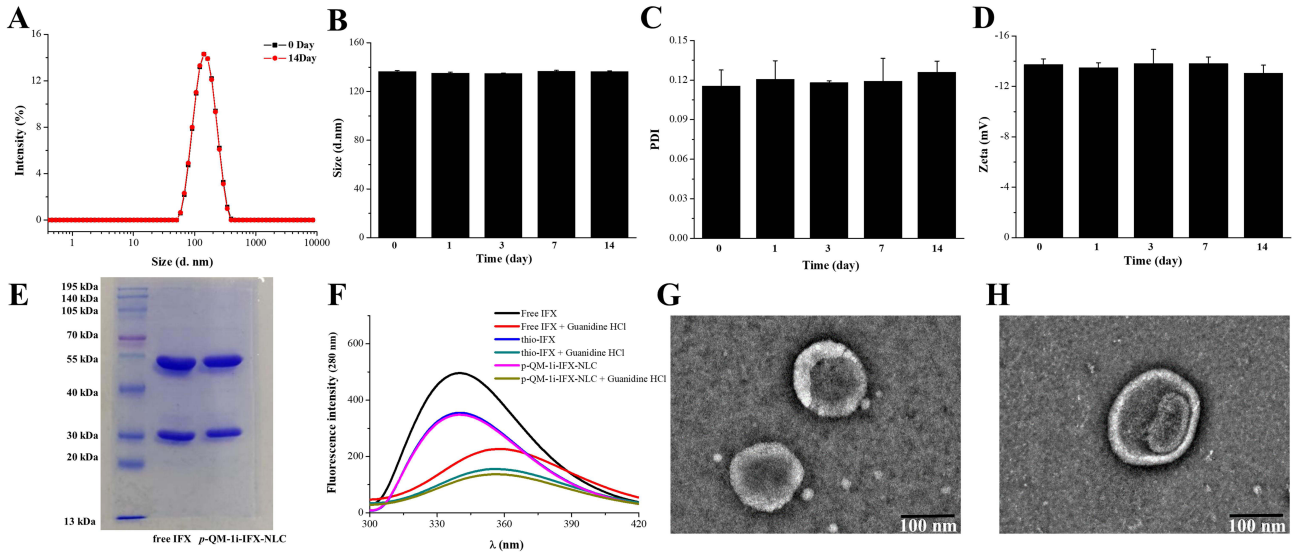

Figure 2 The storage stability of *p*-QM-**1i**-NLC (**A**–**D**), antibody integrity evaluations of IFX antibody on the surface of *p*-QM-**1i**-IFX-NLC (**E** and **F**), and TEM images (**G** and **H**). (**A**) The particle size distribution of *p*-QM-**1i**-NLC on day 0 and day 14. (**B**) Changes in particle size within 14 days. The experiment was performed in triplicate. Error bars represented mean ± SD. (**C**) Changes in PDI within 14 days. The experiment was performed in triplicate. Error bars represented mean ± SD. (**D**) Changes in Zeta within 14 days. The experiment was performed in triplicate. Error bars represented mean ± SD. (**E**) SDS-PAGE of free IFX and *p*-QM-**1i**-IFX-NLC. (**F**) Fluorescence spectroscopy of free IFX, sulfurized IFX and *p*-QM-**1i**-IFX-NLC. (**G**) The TEM image of *p*-QM-**1i**-IFX-NLC. (Scale bar, 100 nm). (**H**) The TEM image of S100-**1i**-IFX-NLC. (Scale bar, 100 nm).

https://doi.org/10.2147/IJN.S548696

intensity at 340.40 ± 0.20 and 340.27 ± 0.42 nm, respectively; and under the action of the guanidine hydrochloride, they also exhibited fluorescence intensity suppression and an increase in the maximum fluorescence emission wavelength (356.60 ± 0.92 and 356.67 ± 0.70 nm). This indicates that the thiolation of IFX and coupling with p-QM-1i-NLC surface did not cause any changes in the tertiary structure of IFX antibodies. In addition, the analysis results of transmission electron microscopy showed that the nanoparticles of *p*-QM-**1i**-IFX-NLC were almost spherical, with a particle size similar to the DLS results of *p*-QM-**1i**-NLC (Figure 2G).

S100-1i-IFX-NLC

Furthermore, in order to overcome the strong environment of the gastrointestinal tract and specific release in the colon, *p*-QM-**1i**-IFX-NLC was coated with Eudragit S100 to prepare orally administered S100-**1i**-IFX-NLC. According to dynamic light scattering analysis, the particle size of S100-**1i**-IFX-NLC was 194.20 nm, PDI was 0.223, and zeta potential was −12.8 mV (Table 1). The transmission electron microscopy images in Figures 2H showed that the nanoparticles of S100-**1i**-IFX-NLC were also almost spherical, with a particle size similar to the DLS results. The particle size of S100-**1i**-IFX-NLC after coating was approximately 58 nm larger than that of *p*-QM-**1i**-IFX-NLC before coating.

Besides, in order to determine whether the nanomaterials had toxic activity, we conducted preliminary cytotoxicity assays on the empty S100-IFX-NLC. As shown in Figure S1, empty S100-IFX-NLC had no significant effect on the cell viability; while, as the concentration of *p*-QM-**1i** increased, the cell viability of S100-**1i**-IFX-NLC decreased. This indicated that the empty S100-IFX-NLC was safe or low toxic.

Study on the Anti-UC Activity in vivo

Effects on Symptoms of UC Mouse Model

DSS-induced UC mice were selected as the experimental model for evaluating oral administration of S100-**1i**-IFX-NLC, which can simulate the disease characteristics of human UC. Balb/c mice were allowed to freely drink 3% DSS aqueous solution to establish the UC model, and drugs was administered orally on the fifth day for treatment (Figure 3A). As shown

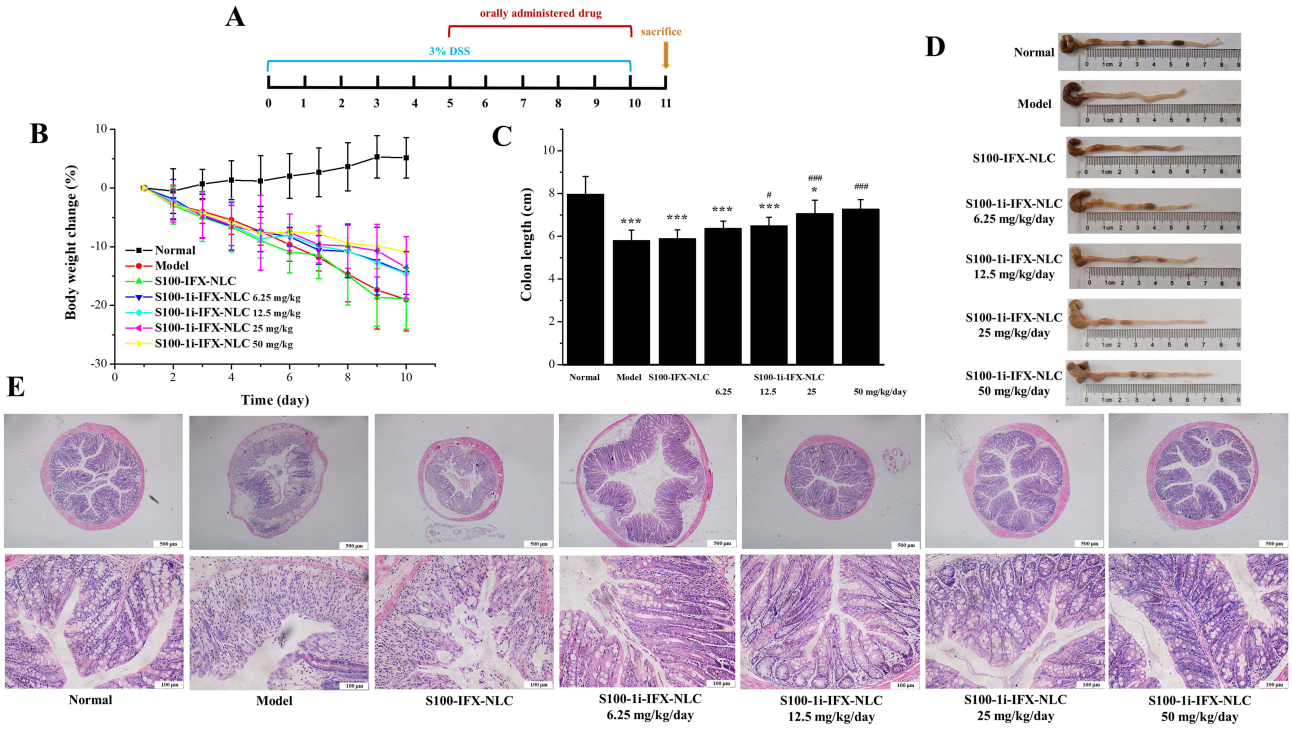

Figure 3 Anti-UC evaluation of S100-**1i**-IFX-NLC in the DSS-induced UC mouse model. (**A**) The experimental time line. (**B**) Body weight changes of different experiment groups (n = 8 for each group). Error bars represented mean ± SD. (**C**) Colon length of different experiment groups (n = 8 for each group). Error bars represented mean ± SD. (**D**) Representative images of colon length. (**E**) Histopathological images of the colon. (Scale bar, 500 μm and 100 μm) *p < 0.05 and ***p < 0.01, compared with the normal group; #p < 0.05 and ###p < 0.001, compared with the model group.

in Figure 3B–E, in the DSS-induced UC mouse model, the efficacy of oral administration S100-**1i**-IFX-NLC was evaluated from multiple aspects, including changes in body weight and colon length, and histopathological analysis of the colon. In the DSS-induced UC mouse model group, there was a significant decrease in body weight, a significant shortening of colon length, and clear acute inflammatory features in colon tissue, such as infiltration of inflammatory cells, structural loss, and disappearance of crypts. Non drug-loaded S100-IFX-NLC had no effect on the intervention of UC mice. While, the intervention of S100-**1i**-IFX-NLC in UC mice can reduce weight loss and colon shortening caused by UC, and resist the acute inflammatory characteristics caused by UC. Among them, only 12.5 mg/kg of S100-**1i**-IFX-NLC had significant anti-UC effects, especially in effectively resisting the acute inflammatory characteristics of colon tissue.

Regulation of Inflammatory Related Proteins in UC Colon Tissues

Following the analysis of acute inflammation characteristics in colonic pathological tissue, we further performed inflammatory analysis on the supernatant of the homogenate of the colon tissues. The TLR4/nuclear factor (NF)-κB signaling pathway is an important inflammatory pathway and a breakthrough point for the prevention and treatment of UC.[34] TLR4, as the main pattern recognition receptor mediating innate immune and inflammatory responses, plays an initiating role in inflammatory responses. NF-κB is a key nuclear factor that triggers and regulates inflammatory responses. Activated NF-κB undergoes nuclear transfer, further promoting the transcription and translation of cytokines such as IL-6, IL-1β, and TNF-α, as well as NLRP3.[35–37] NLRP3 inflammasome plays an extremely important role in immunity and inflammation. The activation of NLRP3 further activates Caspase1, thereby promoting the release of mature IL-1β and facilitating the occurrence and development of inflammatory reactions.[38]

We chose pro-inflammatory cytokines TNF-α and IL-1β, and inflammasome NLRP3 for measurement, using Western blot. As shown in Figure 4A–D, in UC mice of the model group, the expression levels of pro-inflammatory cytokines TNF-α and IL-1β and inflammasome NLRP3 in colon tissue were significantly increased, due to inflammation of UC. The expression levels of TNF-α, IL-1β, and NLRP3 in the colon tissue of the S100-IFX-NLC group were similar to those in the model group. Treatment with 6.25 and 25 mg/kg of S100-**1i**-IFX-NLC can effectively downregulate these inflammatory-related proteins; and 25 mg/kg of S100-**1i**-IFX-NLC can basically reverse these changes. These data indicated that the drug loaded S100-**1i**-IFX-NLC can effectively inhibit inflammation in UC mice.

Effects of Oxidative Stress on UC Mice

MDA, MPO, and CAT are commonly used indicators of oxidative stress. MDA is the final product of lipid peroxidation and an important indicator of oxidative stress.[39] MPO is a peroxidase associated with neutrophils,[40] and changes in its activity can reflect the intensity of inflammatory responses.[41] CAT is a widely present antioxidant enzyme in living organisms that can catalyze the decomposition of hydrogen peroxide into water and oxygen to protect cells from oxidative stress.[42] CAT reflects the body's ability to clear hydrogen peroxide and can be used to evaluate the function of the antioxidant system.

The Nrf2/HO-1 is an important pathway associated with oxidative stress, which can maintain cellular redox homeostasis by regulating the expression of related proteins. Nrf2 is the main regulatory factor of the antioxidant defense system in the body, involved in signal transduction related to various intracellular defense mechanisms. HO-1 is a downstream target protein of Nrf2, which can degrade hemoglobin and release biliverdin, CO, and ferrous ions.

As shown in Figure 4E and F, the MDA content and MPO activity in colon tissue of UC mice in the model group were significantly increased, indicating the generation of oxidative stress. And the S100-IFX-NLC group without drug loading showed no intervention effect on UC mice. Meanwhile, the drug loaded S100-**1i**-IFX-NLC had a significant intervention effect on UC mice, with a significant decrease in MDA content and MPO activity in colon tissue. In addition, as shown in Figure 4G, in the model group and S100-IFX-NLC group, the CAT activity in the colon tissue of UC mice was significantly reduced; the intervention of S100-**1i**-IFX-NLC significantly increased the CAT activity in UC mice. These data indicated that S100-**1i**-IFX-NLC can effectively inhibit oxidative stress caused by UC.

As shown in Figure 4H–J, in the model group, the Nrf2/HO-1 signaling pathway was activated to resist oxidative stress in the colon of UC mice; the expression levels of Nrf2 and HO-1 were significantly increased. Non drug-loaded S100-IFX-NLC treatment group also had higher levels of Nrf2 and HO-1. While, in the S100-**1i**-IFX-NLC groups loaded

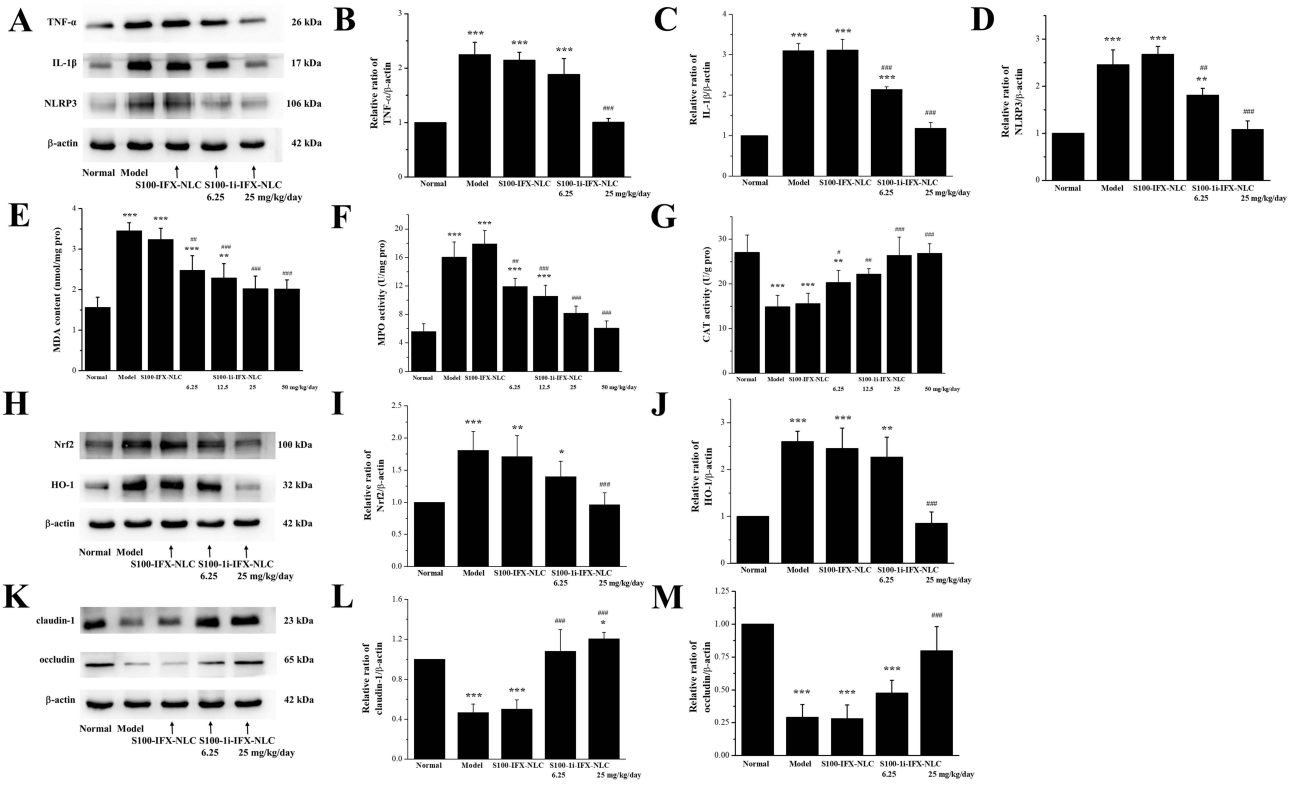

Figure 4 Effects of S100-**1i**-IFX-NLC on inflammation, oxidative stress and tight junctions related proteins in DSS-induced UC mice. (**A**) Representative target protein bands related to inflammation. (**B**) Relative ratio of TNF-α. (**C**) Relative ratio of IL-1β. (**D**) Relative ratio of NLRP3. (**E**) MDA. (n = 8 for each group) (**F**) MPO. (n = 8 for each group) (**G**) CAT. (n = 8 for each group) (**H**) Representative target protein bands related to oxidative stress. (**I**) Relative ratio of Nrf2. (**J**) Relative ratio of HO-1. (**K**) Representative target protein bands related to tight junctions. (**L**) Relative ratio of Claudin-1. (**M**) Relative ratio of occludin. *p < 0.05, **p < 0.01 and ***p < 0.001, compared with the normal group; $^{\#}$p < 0.05, $^{\#\#}$p < 0.01 and $^{\#\#\#}$p < 0.001, compared with the model group. The experiment was performed in triplicate. Error bars represented mean ± SD.

with drugs, the expression levels of Nrf2 and HO-1 decreased, indicating that the intervention of S100-**1i**-IFX-NLC can effectively resist oxidative stress in UC mice.

Effects of Tight Junctions Proteins on Ulcerative Colon

Dysfunction of intestinal barrier leads to increased intestinal permeability, which plays an important role in the pathogenesis of UC.[43–45] Tight junction (TJ) is an important component of the intestinal epithelial barrier, which can regulate the selective permeability of intestinal epithelial disorders, and prevent pathogenic antigens from entering the mucosal lamina propria and causing inflammation and immune reactions in the intestine and surrounding body. TJs mainly exist in the junction complexes between epithelial cells and endothelial cells, bringing adjacent cell membranes together to form a physical barrier structure surrounding the cells. TJ is a complex composed of multiple proteins, including transmembrane proteins, peripheral membrane proteins, and cytoskeletal proteins.[46] Transmembrane proteins include the following three intact membrane proteins: junctional adhesion molecule, occludin, and claudins. Currently, it is believed that occludin and claudins play a major role in transmembrane proteins.

We chose occludin and claudin-1 for measurement, using Western blot. As shown in Figure 4K–M, in the UC mice of the model group, the expression levels of claudin-1 and occludin in the colon tissue were significantly lower than those in normal mice, indicating an increase in intestinal permeability in the colon of UC mice. The intervention of S100-**1i**-IFX-NLC in UC mice can effectively increase the expression levels of claudin-1 and occludin. However, only S100-IFX-NLC did not have such an effect. These results indicated that S100-**1i**-IFX-NLC can also exert anti-UC effects by increasing the levels of TJ proteins (claudin-1 and occludin) to restore intestinal barrier permeability.

Targeted Evaluation of S100-1i-IFX-NLC in vitro and in vivo

The Drug Release Studies of S100-1i-IFX-NLC in vitro

To verify whether S100 coating can achieve specific release in the colon, further in vitro drug release studies of S100-**1i**-IFX-NLC were conducted. Adopting the preparation method of gastric juice, small intestine fluid, and colon fluid in the Chinese Pharmacopoeia. As shown in Figure 5A, S100-**1i**-IFX-NLC did not release *p*-QM-**1i** in artificial gastric juice for 2 hours and artificial small intestine fluid for 3 hours; and when replaced with an artificial colon, *p*-QM-**1i** begins to release.

Targeted Study of Inflammatory Cell Model in vitro

Macrophages play a crucial role in inflammation.[47,48] LPS is widely used as an inducer of macrophage inflammation. The LPS-induced Raw264.7 macrophages cell model is a commonly used inflammatory model, in which TNF-α is highly expressed.[7,49,50]

To verify the targeting of TNF-α on inflammatory cells by IFX modified on the surface of NLC, Cy5.5 labeling was performed on IFX-NLC. One-milligram DSPE-PEG2000 in the experimental method was replaced by 1 mg Cy5.5-DSPE-PEG2000, allowing Cy5.5-IFX-NLC to be detected by fluorescence. As shown in Figure 5B, in the blank group, only the blue fluorescence of DAPI can be observed in cell morphology, which was used to stain the nucleus. In the Cy5.5-IFX-NLC group, in addition to nuclei labeled with DAPI, red fluorescence of Cy5.5 can also be observed in cell morphology. In the Cy5.5-NLC group, only blue fluorescence could be observed in cell morphology, and no red fluorescence could be observed. In Figure 5C, low fluorescence was detected in the samples of the blank group and Cy5.5-NLC group by flow cytometry; And high fluorescence was detected in the samples of Cy5.5-IFX-NLC group. These data indicated that the modification of IFX on Cy5.5-IFX-NLC can effectively target TNF-α in inflammatory cells, resulting in a strong red fluorescence in this cell group.

Fluorescence Imaging Study and HPLC Study of Active Targeting in UC Mice

To determine the active targeting of S100-**1i**-IFX-NLC in vivo, we performed fluorescence imaging qualitative analysis on the colon after oral administration of Cy5.5-S100-IFX-NLC, and quantitatively analyzed the *p*-QM-**1i** content absorbed by the colon after oral administration of S100-**1i**-IFX-NLC (Figure 5D and E).

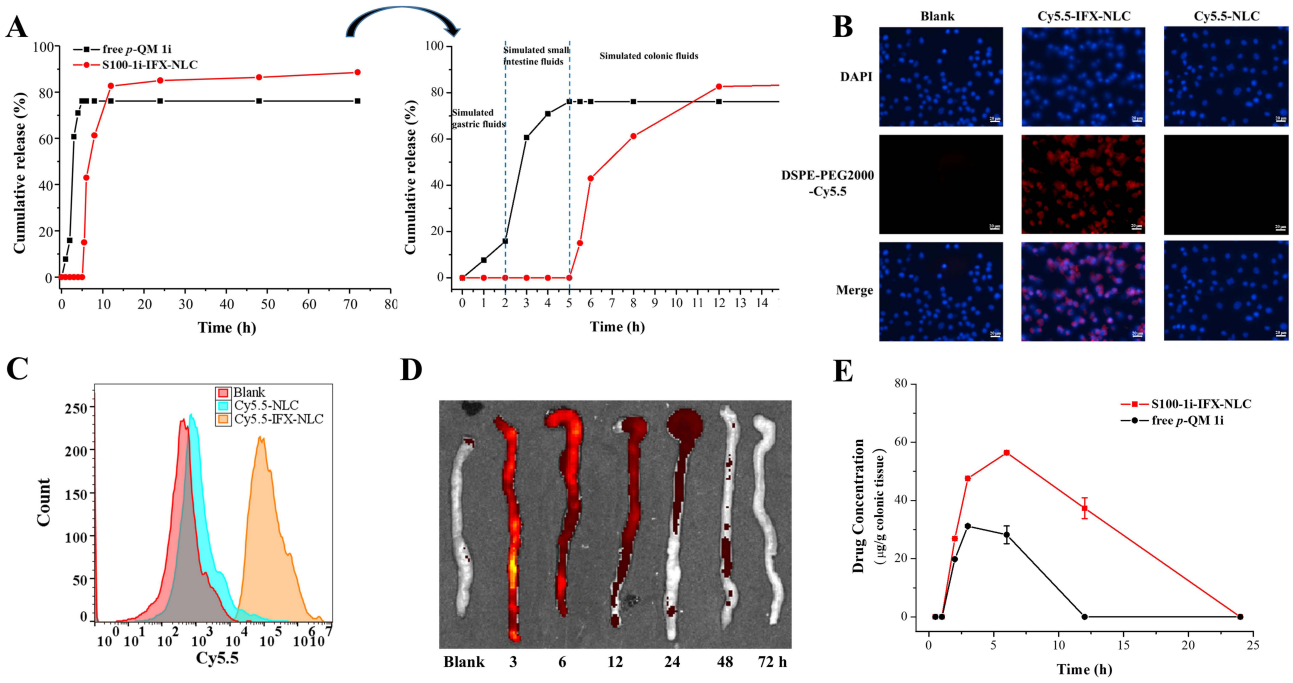

Figure 5 Targeted study of S100-**1i**-IFX-NLC in vitro and in vivo. (**A**) In vitro drug release study of S100-**1i**-IFX-NLC in artificial gastric fluid, small intestinal fluid and colonic fluid. (**B** and **C**) Targeted study in LPS-induced inflammatory cell model of Raw264.7 macrophages using fluorescence microscopy and flow cytometry. (B, scale bar, 20 μm) (**D** and **E**) Targeted studies were conducted using in vivo imaging systems and high performance liquid chromatography (HPLC) in the DSS-induced UC mouse models. The experiment was performed in triplicate. Error bars represented mean ± SD.

https://doi.org/10.2147/IJN.S548696

In the DSS-induced UC mouse model, after oral administration of Cy5.5-S100-IFX-NLC, significant red fluorescence was detected in the colon of UC mice at 3 and 6 hours; as time increases, the intensity of red fluorescence weakened. In addition, as shown in Figure S2, fluorescence imaging of the mouse gastrointestinal tract showed that at 3 hours, the fluorescence in the latter half of the small intestine and colon was stronger than that in the stomach and the first half of small intestine. This was mainly due to the gradual transition of pH in the gastrointestinal tract of mice from strongly acidic (stomach) to neutral/weakly alkaline (intestine), which was different from the completely different pH values between gastric juice, small intestine fluid, and colon fluid used in in vitro drug release experiments.

In the DSS-induced UC mouse model, *p*-QM-**1i** can be detected in the colon tissue homogenate extract after oral administration of S100-**1i**-IFX-NLC for 2 hours. At 6 hours, the content of p-QM-**1i** in the colon reached a high level; and the content of *p*-QM-**1i** in the colon after oral administration of S100-**1i**-IFX-NLC was about twice that of the colon after oral administration of free *p*-QM-**1i**. After oral administration of S100-**1i**-IFX-NLC for 12 hours, the content of *p*-QM-**1i** in the colon decreased; however, after 12 hours of oral administration of free *p*-QM-**1i**, *p*-QM-**1i** was no longer detected in the colon.

Safety Evaluation

We conducted safety assessments of S100-**1i**-IFX-NLC by detecting serum indicators, histopathology, and organ indices. In the DSS-induced UC mouse model, DSS not only causes UC but also penetrates the mucosal epithelial layer and aggregates in other tissues due to the disruption of the intestinal mucosal barrier, resulting in damage to other tissues.[51] AST and ALT in serum are clinical indicators reflecting liver injury; BUN and CRE in serum are indicators reflecting kidney injury.

In DSS-induced UC mice, when DSS accumulated in the liver and kidneys, causing liver and kidney damage, the levels of AST, ALT, BUN and CRE in the serum would increase, as shown in the model group of Figure 6A–D. There was no significant difference in these four serum indicators between the S100-IFX-NLC group and the model group, indicating no statistical significance. The intervention of S100-**1i**-IFX-NLC in UC mice can significantly reduce the levels of serum AST, ALT, BUN and CRE caused by DSS. However, there were no significant differences in histopathological analysis (Figure 6E) and organ indices (Table 2) of the liver, spleen and kidney among the experimental groups. This may be related to the short duration of the UC experiment in the mouse, so abnormalities in serum biochemical indicators were detected first, without detecting changes in organ tissue morphology.

Discussion

Low water-soluble drugs lead to low bioavailability and reduced therapeutic efficacy, so it is usually necessary to increase the dosage of drugs to improve their efficacy; but increasing the dosage will lead to more side effects. In order to address the low water solubility of drugs, nanomedicine delivery systems have emerged. Compared with other types of nanomaterials (polymers, inorganic materials), lipid nanocarriers have extremely low toxicity and immunogenicity.[52–54] NLC evolved from SLN and is composed of a mixture of solid and liquid lipids. Due to the interference of liquid lipids with the regular arrangement of solid lipids, leading to the formation of lattice defect structures, which enables NLC to load more drugs and reduce drug leakage.[55]

We first loaded the active anti-inflammatory lead compound *p*-QM-**1i** with NLC to prepare *p*-QM-**1i**-NLC, in order to increase the solubility of *p*-QM-**1i**. In addition, the preparation of *p*-QM-**1i**-NLC required the selection of suitable liquid lipids, Miglyol 812N, to increase the EE value of the drug. Miglyol 812N had a high solubility for *p*-QM-**1i** (Table S4) and can effectively increase the EE value of *p*-QM-**1i**. For example, when Miglyol 812N was used as a liquid lipid, the EE value of *p*-QM-**1i** in *p*-QM-**1i**-NLC was 86.51%; when Oleic acid was used as a liquid lipid, the EE value of *p*-QM-**1i** in *p*-QM-**1i**-NLC is 62.52% (Table S5). And Miglyol 812N had lower costs.

PEG-2000 modified lipids (DSPE-PEG2000) were used to construct NLCs, which can increase the hydrophilicity of NLCs, reduce their uptake by the reticuloendothelial system, and prolong the circulation time of drugs in the blood.[56–58] In addition, by functionalizing PEG-2000 modified lipids (DSPE-PEG2000-MAL), antibodies can be attached to the surface of NLC, giving NLC active targeting and forming immune NLC. In the treatment research for inflammatory bowel disease, various antigens or receptors, mannose, folate, chemokine receptors, etc. have been applied for active

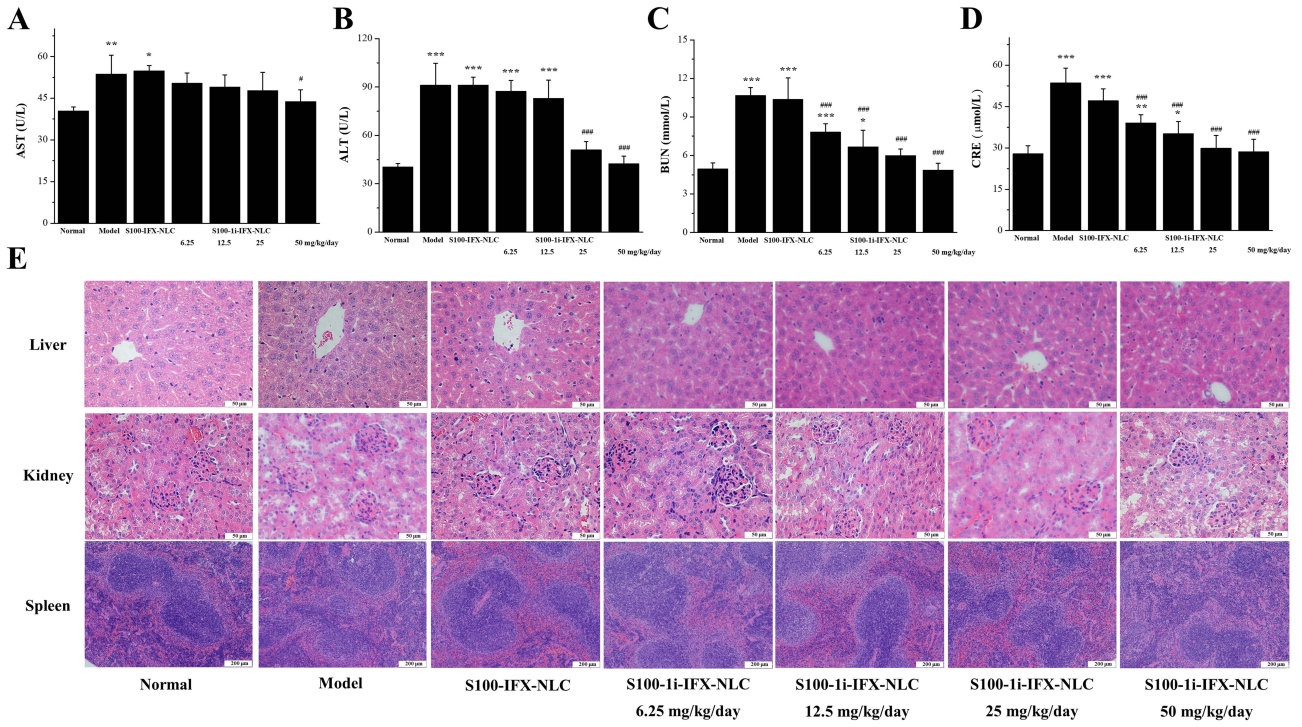

Figure 6 Serum biochemical indicators and histopathological study related to tissue damage in the DSS-induced UC mouse model. (**A**) Serum AST. (**B**) Serum ALT. (**C**) Serum BUN. (**D**) Serum CRE. (n = 8 for each group). The experiment was performed in triplicate. Error bars represented mean ± SD. *p < 0.05, **p < 0.01 and ***p < 0.01, compared with the normal group; $^{\#}$p < 0.05, and $^{\#\#\#}$p < 0.001, compared with the model group. (**E**) Histopathological analysis of liver, kidney, and spleen. (Scale bar, liver 50 μm, kidney 50 μm, spleen 200 μm).

targeting studies.[59] Antibody modified immune NLCs have extremely high targeting specificity, which cannot be compared to other targeting designs. For example, antibody modification is similar to "opening a lock with a key", and mannose modification is similar to "one key can open multiple similar locks"; and the binding between antibodies and antigens is high affinity, while the binding between mannose and receptors is weak.

Furthermore, IFX was modified on the surface of *p*-QM-**1i**-NLC to prepare *p*-QM-**1i**-IFX-NLC, which can actively target TNF-α highly expressed in inflammatory cells or tissues. DSPE-PEG2000-Mal with a molar ratio of 0.1% of the total lipids was used as the lipid for connecting the antibody on the surface of *p*-QM-**1i**-NLC. And compared with other literature,[23] the molar ratio of IFX to DSPE-PEG2000-Mal was reduced to 1.5:1, but the antibody conjugation efficiency could be maintained at 90%. Minimize the use of DSPE-PEG2000-Mal and IFX for the preparation of *p*-QM-**1i**-IFX-NLC, which can reduce the amount of IFX used and only maintain its active targeting effect, and minimize costs as much as possible.

The *p*-QM-**1i**-NLC surface is modified with IFX, which can actively target highly expressed TNF-α in inflammatory cells or tissues. However, when these antibodies modified nanoparticles are exposed to the gastrointestinal tract, the antibodies are easily destroyed.[60] Therefore, *p*-QM-**1i**-IFX-NLC is coated with Eudragit S100 to prepare S100-**1i**-IFX-

Table 2 Organ Indexes of Liver and Kidney of DSS-Induced Mice

Groups	Liver	Kidney	Spleen
Control	0.0454 ± 0.0020	0.0145 ± 0.00042	0.00536 ± 0.00079
Model	0.0456 ± 0.0033	0.0148 ± 0.00041	0.00531 ± 0.00043
S100-IFX-NLC	0.0476 ± 0.0031	0.0148 ± 0.00054	0.00542 ± 0.00034
6.25 mg/kg S100-1i-IFX-NLC	0.0463 ± 0.0031	0.0143 ± 0.00050	0.00545 ± 0.00099
12.5 mg/kg S100-1i-IFX-NLC	0.0467 ± 0.0022	0.0147 ± 0.00052	0.00509 ± 0.00022
25 mg/kg S100-1i-IFX-NLC	0.0461 ± 0.0029	0.0146 ± 0.00119	0.00521 ± 0.00047
50 mg/kg S100-1i-IFX-NLC	0.0469 ± 0.0014	0.0141 ± 0.00044	0.00516 ± 0.00059

https://doi.org/10.2147/IJN.S548696

NLC, which can protect S100-**1i**-IFX-NLC from interference from the gastrointestinal environment and achieve specific release of *p*-QM-**1i**-IFX-NLC in the colon.

The design of S100-**1i**-IFX-NLC includes a dual-stage targeted colon design. One is S100 coating that can be orally administered and specifically released in the colon; secondly, IFX monoclonal antibodies are modified on the surface of *p*-QM-**1i**-NLC to target the highly expressed transmembrane TNF-α in inflamed colon tissue.

The in vitro drug release study of S100-**1i**-IFX-NLC found that *p*-QM-**1i** can be effectively released in artificial colon fluid but not in artificial gastric and small intestine fluid. This suggested that the in vitro drug release of S100-**1i**-IFX-NLC was pH dependent; and the design of S100 coating on the surface of *p*-QM-**1i**-IFX-NLC can protect S100-**1i**-IFX-NLC from strong environmental interference in the gastrointestinal tract and achieve specific release to the colon.

In the inflammatory Raw264.7 cells model, fluorescence labeled and IFX modified Cy5.5-IFX-NLC can effectively target TNF-α through qualitative fluorescence morphology and quantitative flow cytometry analysis. In the UC mouse model, fluorescence in vivo imaging experiments showed that Cy5.5-S100-IFX-NLC can effectively aggregate in the lesion colon tissue; and the quantitative experiment determined by HPLC also showed that S100-**1i**-IFX-NLC can effectively aggregate in the lesion colon tissue; it not only increased the content of *p*-QM-**1i** in colon tissue but also prolonged the duration of *p*-QM-**1i** action. The targeted studies in vitro and in vivo suggested that the dual-stage targeted design of IFX modification and S100 coating on NLC can effectively increase the targeting of the inflammatory colon, causing *p*-QM-**1i** to aggregate in the diseased colon, increasing drug concentration, and prolonging drug action time.

For the anti-UC activity in the UC mice model, 25 or 50 mg/kg of S100-**1i**-IFX-NLC can effectively resist DSS-induced colon length shortening and acute inflammatory damage to UC tissue. In our previous work,[7] 50 mg/kg of free *p*-QM-**1i** was not effective in resisting UC injury, and 200 mg/kg of free *p*-QM **1i** was needed to effectively inhibit UC injury (effectively suppressing colon shortening and inflammatory pathological changes in colon tissue of UC mice). This suggested that the design of S100-**1i**-IFX-NLC can significantly reduce the usage of *p*-QM-**1i**, which should be related to the increased solubility of *p*-QM-**1i** and the achievement of targeted colonic release of drugs. In addition, the reduction of *p*-QM-**1i** usage can effectively reduce the side effects caused by the drug.

Inflammation is a prominent pathological feature of UC.[61] Oxidative stress is a stress state caused by an imbalance between the oxidative and antioxidant systems, which plays a crucial role in the occurrence of UC.[62,63] Under normal physiological conditions, reactive oxygen species (ROS) and reactive nitrogen species (RNS) are produced at moderate concentrations. However, under oxidative stress conditions, excessive ROS and RNS are produced, exacerbating the inflammatory response.[64–66] Intestinal barrier dysfunction is not only a result of UC but also a key driving factor in its occurrence and development. Further mechanistic studies have found that S100-1i-IFX-NLC can exert its anti-UC activity by suppressing inflammation, oxidative stress and intestinal barrier dysfunction.

Safety evaluation is a necessary prerequisite for the clinical translation of drugs and medical nanomaterials. Through active targeting, NLC can reduce the non-specific distribution of drugs, increase drug accumulation in colon lesions, and improve the safety and efficacy of treatment. In the study of anti-UC activity in vivo, 25 or 50 mg/kg of S100-**1i**-IFX-NLC could effectively resist DSS-induced UC injury. While, 200 mg/kg of free *p*-QM-**1i** was needed to effectively inhibit UC injury in previous study.[7] The design of S100-**1i**-IFX-NLC can reduce the dosage of drug and correspondingly decrease the toxic side effects of the drug.

For safety evaluation research in UC mice, due to the disruption of the intestinal mucosal barrier, DSS penetrates the mucosal epithelial layer and aggregates in other organs, leading to organ damage. The detection of serum biochemical indicators showed that S100-**1i**-IFX-NLC can effectively protect the liver and kidneys of mice against organ damage caused by UC.

Conclusion

In conclusion, the dual-stage targeted design of S100-**1i**-IFX-NLC can effectively increase the solubility of *p*-QM-**1i**, allowing S100-**1i**-IFX-NLC to target the colon and *p*-QM-**1i**-IFX-NLC to target the inflammatory tissue, increasing the aggregation of *p*-QM-**1i** in the colon, enhancing the efficacy of *p*-QM-**1i**, reducing the usage of *p*-QM-**1i**, and increasing safety. The oral and targeted anti-UC nanomedicine S100-**1i**-IFX-NLC and its dual-stage targeted design are valuable and worthy of further research.

Data Sharing Statement

Data will be provided by the corresponding author (Jie Yang) as required.

Funding

This work was supported by Shandong Provincial Natural Science Foundation (ZR2023MB089) and the Research Fund of Liaocheng University (318012106).

Disclosure

The authors declare that they have no conflicts of interest in this work.

References

1. Adams SM, Bornemann PH. Ulcerative colitis. *Am Fam Physician*. 2013;87:699–705.
2. Saleh M, Trinchieri G. Innate immune mechanisms of colitis and colitis-associated colorectal cancer. *Nat Rev Immunol*. 2011;11:9–20. doi:10.1038/nri2891
3. Xue JC, Yuan S, Meng H, et al. The role and mechanism of flavonoid herbal natural products in ulcerative colitis. *Biomed Pharmacother*. 2023;158:114086. doi:10.1016/j.biopha.2022.114086
4. Ordas I, Eckmann L, Talamini M, Baumgart DC, Sandborn WJ. Ulcerative colitis. *Lancet*. 2012;380:1606–1619. doi:10.1016/S0140-6736(12)60150-0
5. Kula K, Nagatsky R, Sadowski M, Siumka Y, Demchuk OM. Arylcyanomethylenequinone oximes: an overview of synthesis, chemical transformations, and biological activity. *Molecules*. 2023;28:5229. doi:10.3390/molecules28135229
6. Li PX, Ma YZ, Wang K, Shi XH, Yang J, Liu GY. Design, synthesis and antitumor activity of potent and safe *para*-quinone methides derivatives in vitro and in vivo. *Biomed Pharmacother*. 2022;156:113893. doi:10.1016/j.biopha.2022.113893
7. Qiu Y, Li X, Zhang X, et al. Anti-inflammatory effects of *para*-quinone methide derivatives on ulcerative colitis. *Front Pharmacol*. 2024;15:1474678. doi:10.3389/fphar.2024.1474678
8. Mall J, Naseem N, Haider MF, Rahman MA, Khan S, Siddiqui SN. Nanostructured lipid carriers as a drug delivery system: a comprehensive review with therapeutic applications. *Intell Pharma*. 2025;3:243–255.in press. doi:10.1016/j.ipha.2024.09.005
9. Nguyen VH, Thuy VN, Van TV, Dao AH, Lee BJ. Nanostructured lipid carriers and their potential applications for versatile drug delivery via oral administration. *OpenNano*. 2022;8:100064.
10. Beloqui A, Del Pozo-Rodríguez A, Isla A, Rodríguez-Gascón AA, Solinís MÁ. Nanostructured lipid carriers as oral delivery systems for poorly soluble drugs. *J Drug Deliv Sci Tec*. 2017;42:144–154.
11. Jaiswal P, Gidwani B, Vyas A. Nanostructured lipid carriers and their current application in targeted drug delivery. *Artif Cell Nanomed B*. 2016;44:27–40.
12. Zu MH, Ma Y, Cannup B, et al. Oral delivery of natural active small molecules by polymeric nanoparticles for the treatment of inflammatory bowel diseases. *Adv Drug Deliv Rev*. 2021;176:113887. doi:10.1016/j.addr.2021.113887
13. Mitragotri S, Burke PA, Langer R. Overcoming the challenges in administering biopharmaceuticals: formulation and delivery strategies. *Nat Rev Drug Discov*. 2014;13:655e72. doi:10.1038/nrd4363
14. Zelikin AN, Ehrhardt C, Healy AM. Materials and methods for delivery of biological drugs. *Nat Chem*. 2016;8:997e1007.
15. Janrao C, Khopade S, Bavaskar A, Sudhakar Gomte S, Agnihotri TG, Jain A. Recent advances of polymer based nanosystems in cancer management. *J Biomater Sci Polym Ed*. 2023;34:1274–1335. doi:10.1080/09205063.2022.2161780
16. Ibekwe VC, Fadda HM, Mcconnell EL, Khela MK, Evans DF, Basit AW. Interplay between intestinal pH, transit time and feed status on the in vivo performance of pH responsive ileo-colonic release systems. *Pharm Res-Dordr*. 2008;25:1828–1835.
17. Ashford M, Fell T. Targeting drugs to the colon: delivery systems for oral administration. *J Drug Targeting*. 1994;2:241–258.
18. Koziolek M, Grimm M, Becker D, et al. Investigation of pH and temperature profiles in the GI tract of fasted human subjects using the Intellicap® system. *J Pharm Sci*. 2015;104(9):2855–2863. doi:10.1002/jps.24274
19. Rehman S, Ranjha NM, Shoukat H, et al. Fabrication, evaluation, in vivo pharmacokinetic and toxicological analysis of pH-sensitive eudragit S-100-coated hydrogel beads: a promising strategy for colon targeting. *AAPS Pharm Sci Tech*. 2021;22:1–17. doi:10.1208/s12249-021-02082-y
20. Sunoqrot S, Abujamous L. pH-sensitive polymeric nanoparticles of quercetin as a potential colon cancer-targeted nanomedicine. *J Drug Deliv Sci Tec*. 2019;52:670–676.
21. Liu X, Zhang MY, Tian YX, et al. Development, characterization, and investigation of in vivo targeted delivery efficacy of luteolin-loaded, eudragit S100-coated mPEG-PLGA nanoparticles. *AAPS Pharm Sci Tech*. 2022;23:100. doi:10.1208/s12249-022-02255-3
22. Trisopon K, Saokham P, Kittipongpatana N, Chomchoei N, Kittipongpatana OS. Development of a multifunctional rice starch-based co-processed excipient for direct compression and colon-targeted drug delivery. *J Drug Deliv Sci Tec*. 2025;112:107279. doi:10.1016/j.jddst.2025.107279
23. Matusewicz L, Filip-Psurska B, Psurski M, et al. EGFR-targeted immunoliposomes as a selective delivery system of simvastatin, with potential use in treatment of triple-negative breast cancers. *Int Pharmaceut*. 2019;569:118605.
24. Josimar OE, Raquel P, Deise LC, Fabiano PS, Robert JL, Juliana MM. Anti-HER2 immunoliposomes for co-delivery of paclitaxel and rapamycin for breast cancer therapy. *Eur J Pharm Biopharm*. 2017;115:159–167. doi:10.1016/j.ejpb.2017.02.020
25. Raquel P, Josimar OE, Renata FVL, Robert JL. Cetuximab immunoliposomes enhance delivery of 5-FU to skin squamous carcinoma cells. *Anticancer Agents Med Chem*. 2017;17:301–308. doi:10.2174/1871520616666160526110913
26. Qin HY, Xiao HT, Wu JC, Berman BM, Sun JJ, Bian ZX. Key factors in developing the trinitrobenzene sulfonic acid-induced post-inflammatory irritable bowel syndrome model in rats. *World J Gastroenterol*. 2012;18:2481–2492. doi:10.3748/wjg.v18.i20.2481

27. Petrilli R, Eloy JO, Saggioro FP, et al. Skin cancer treatment effectiveness is improved by iontophoresis of EGFR-targeted liposomes containing 5-FU compared with subcutaneous injection. *J Control Release*. 2018;283:151–162. doi:10.1016/j.jconrel.2018.05.038
28. Zalba S, Contreras AM, Haeri A, et al. Cetuximab-oxaliplatin-liposomes for epidermal growth factor receptor targeted chemotherapy of colorectal cancer. *J Control Release*. 2015;210:26–38. doi:10.1016/j.jconrel.2015.05.271
29. Zhao L, Wang F, Cai ZW, et al. Improving drug utilization platform with injectable mucoadhesive hydrogel for treating ulcerative colitis. *Chem Eng J*. 2021;424:130464. doi:10.1016/j.cej.2021.130464
30. Lee SH, Song JG, Han HK. Site-selective oral delivery of therapeutic antibodies to the inflamed colon via a folic acid grafted organic/inorganic hybrid nanocomposite system. *Acta Pharm Sin B*. 2022;12:4249–4261. doi:10.1016/j.apsb.2022.06.006
31. Li PX, Guo XY, Liu T, Liu Q, Yang J, Liu GY. Evaluation of hepatoprotective effects of piperlongumine derivative PL 1-3-Loaded albumin nanoparticles on lipopolysaccharide/D-galactosamine-induced acute liver injury in mice. *Mol Pharm*. 2022;19:4576–4587.
32. Eftink MR. The use of fluorescence methods to monitor unfolding transitions in proteins. *Biochemistry*. 1994;63:276–284.
33. Eloy JO, Ruiz A, Lima FTD, et al. EGFR-targeted immunoliposomes efficiently deliver docetaxel to prostate cancer cells. *Colloid Surf B*. 2020;194:111185. doi:10.1016/j.colsurfb.2020.111185
34. Li Y, Pan X, Yin M, Li C, Han L. Preventive effect of lycopene in dextran sulfate sodium-induced ulcerative colitis mice through the regulation of TLR4/TRIF/NF-kappaB signaling pathway and tight junctions. *J Agric Food Chem*. 2021;69:13500–13509. doi:10.1021/acs.jafc.1c05128
35. Zhu LB, Gong XY, Gong JP, et al. Notoginsenoside R1 upregulates miR-221-3p expression to alleviate ox-LDL-induced apoptosis, inflammation, and oxidative stress by inhibiting the TLR4/NF-κB pathway in HUVECs. *Braz J Med Biol Res*. 2020;53:e9346.
36. Kim YS, Ahn CB, Je YJ. Anti-inflammatory action of high molecular weight Mytilus edulis hydrolysates fraction in LPS-induced RAW264.7 macrophage via NF-kappaB and MAPK pathways. *Food Chem*. 2016;202:9–14. doi:10.1016/j.foodchem.2016.01.114
37. Hwang PA, Chien SY, Chan YL, et al. Inhibition of Lipopolysaccharide (LPS) induced inflammatory responses by Sargassum hemiphyllum sulfated polysaccharide extract in RAW 264.7 macrophage cells. *J Agric Food Chem*. 2011;59:2062–2068. doi:10.1021/jf1043647
38. Kelley N, Jeltema D, Duan Y, He Y. The NLRP3 inflammasome: an overview of mechanisms of activation and regulation. *Int J Mol Sci*. 2019;20:3328. doi:10.3390/ijms20133328
39. Jentzsch AM, Bachmann H, Furst P, Biesalski HK. Improved analysis of malondialdehyde in human body fluids. *Free Radic Biol Med*. 1996;20:251–256. doi:10.1016/0891-5849(95)02043-8
40. Palla AH, Iqbal NT, Minhas K, Gilani AH. Flaxseed extract exhibits mucosal protective effect in acetic acid induced colitisin mice by modulating cytokines, antioxidant and anti-inflammatory mechanisms. *Int Immunopharmacol*. 2016;38:153–166. doi:10.1016/j.intimp.2016.04.043
41. Bo L, Shan JG, Zhao ZW. Research progress of myeloperoxidase in cardiovascular diseases. *Lab Med*. 2017;32:738–743.
42. Sepasi Tehrani H, Moosavi-Movahedi AA. Catalase and its mysteries. *Prog Biophys Mol Biol*. 2018;140:5–12. doi:10.1016/j.pbiomolbio.2018.03.001
43. Danese S, Fiocchi C. Ulcerative colitis. *N Engl J Med*. 2011;365:1713–1725. doi:10.1056/NEJMra1102942
44. Pope JL, Bhat AA, Sharma A, et al. Claudin-1 regulates intestinal epithelial homeostasis through the modulation of Notch-signaling. *Gut*. 2014;63:622–632. doi:10.1136/gutjnl-2012-304241
45. Kiesler P, Fuss IJ, Strober W. Experimental models of inflammatory bowel diseases. *Cell Mol Gastroenterol Hepatol*. 2015;1:154–170. doi:10.1016/j.jcmgh.2015.01.006
46. Turner JR. Intestinal mucosal barrier function in health and disease. *Nat Rev Immunol*. 2009;9:799–809. doi:10.1038/nri2653
47. Chawla A, Nguyen KD, Goh YP. Macrophage-mediated inflammation in metabolic disease. *Nat Rev Immunol*. 2011;11:738–749. doi:10.1038/nri3071
48. Fries W, Cottone M, Cascio A. Systematic review: macrophage activation syndromein inflammatory bowel disease. *Aliment Pharmacol Ther*. 2013;37:1033–1045. doi:10.1111/apt.12305
49. Ma YZ, Guo XY, Wang Q, et al. Anti-inflammatory effects of β-ionone-curcumin hybrid derivatives against ulcerative colitis. *Chem Biol Interact*. 2022;367:110189. doi:10.1016/j.cbi.2022.110189
50. Ren ZY, Zhang X, Li X, Wang XT, Yang J, Liu GY. Design, synthesis and biological evaluation of diarylmethyl amine derivatives with anti-ulcerative colitis activity via inhibiting inflammation and oxidative stress. *Eur J Med Chem*. 2025;289:117433. doi:10.1016/j.ejmech.2025.117433
51. Yang CH, Merlin D. Unveiling colitis: a journey through the dextran sodium sulfate-induced model. *Inflamm Bowel Dis*. 2024;30:844–853. doi:10.1093/ibd/izad312
52. Müller RH, Mäder K, Gohla S. Solid lipid nanoparticles (SLN) for controlled drug delivery – a review of the state of the art. *Eur J Pharm Biopharm*. 2000;50:161–177. doi:10.1016/S0939-6411(00)00087-4
53. Akel H, Ismail R, Katona G, Sabir F, Ambrus R, Csóka I. A comparison study of lipid and polymeric nanoparticles in the nasal delivery of meloxicam: formulation, characterization, and in vitro evaluation. *Int J Pharm*. 2021;604:120724. doi:10.1016/j.ijpharm.2021.120724
54. Ghasemiyeh P, Mohammadi-Samani S. Solid lipid nanoparticles and nanostructured lipid carriers as novel drug delivery systems: applications, advantages and disadvantages. *Res Pharm Sci*. 2018;13:288. doi:10.4103/1735-5362.235156
55. Haider M, Abdin SM, Kamal L, Orive G. Nanostructured lipid carriers for delivery of chemotherapeutics: a review. *Pharmaceutics*. 2020;12:288. doi:10.3390/pharmaceutics12030288
56. Moghimi SM, Hunter AC, Murray JC. Long-circulating and target-specific nanoparticles: theory to practice. *Pharmacol Rev*. 2001;53:283–318.
57. Liu YF, Liang YS, J Y, et al. Advances in nanotechnology for enhancing the solubility and bioavailability of poorly soluble drugs. *Drug Des Dev Ther*. 2024;18:1469–1495. doi:10.2147/DDDT.S447496
58. Zhu Q, Chen ZJ, Paul PK, Lu Y, Wu W, Qi JP. Oral delivery of proteins and peptides: challenges, status quo and future perspectives. *Acta Pharm Sin B*. 2021;11:2416–2448. doi:10.1016/j.apsb.2021.04.001
59. Gao J, Li JN, Luo ZY, Wang HY, Ma ZM. Nanoparticle-based drug delivery systems for inflammatory bowel disease treatment. *Drug Des Dev Ther*. 2024;18:2921–2949. doi:10.2147/DDDT.S461977
60. Joseph SK, Sabitha M, Nair SC. Stimuli-responsive polymeric nanosystem for solon specific drug delivery. *Adv Pharm Bull*. 2020;10:1–12. doi:10.15171/apb.2020.001
61. Cleveland NK, Torres J, Rubin DT. What does disease progression look like in ulcerative colitis, and how might it be prevented? *Gastroenterology*. 2022;162:1396–1408. doi:10.1053/j.gastro.2022.01.023

62. Dudzińska E, Gryzinska M, Ognik K, Gil-Kulik P, Kocki J. Oxidative stress and effect of treatment on the oxidation product decomposition processes in IBD. *Oxid Med Cell Longev*. 2018;7918261. doi:10.1155/2018/7918261
63. Tsopmejio ISN, Yuan J, Diao Z, et al. Auricularia polytricha and flammulina velutipes reduce liver injury in DSS-induced inflammatory bowel disease by improving inflammation, oxidative stress, and apoptosis through the regulation of TLR4/NF-κB signaling pathways. *J Nutr Biochem*. 2023;111:109190. doi:10.1016/j.jnutbio.2022.109190
64. Lei Y, Wang K, Deng L, Chen Y, Nice EC, Huang C. Redox regulation of inflammation: old elements, a new story. *Med Res Rev*. 2015;35:306–340. doi:10.1002/med.21330
65. Yu J, Yao H, Gao X, Zhang Z, Wang JF, Xu SW. The role of nitric oxide and oxidative stress in intestinal damage induced by selenium deficiency in chickens. *Biol Trace Elem Res*. 2015;163:144–153. doi:10.1007/s12011-014-0164-8
66. Mittal M, Siddiqui MR, Tran K, Reddy SP, Malik AB. Reactive oxygen species in inflammation and tissue injury. *Antioxid Redox Sign*. 2014;20:1126–1167. doi:10.1089/ars.2012.5149